Cell Death and Differentiation (2007) 14, 1880–1892
© 2007 Nature Publishing Group All rights reserved 1350-9047/07 $30.00
www.nature.com/cdd

Bcl-X_L modulates the differentiation of immortalized human neural stem cells

I Liste*[,1,2], E García-García[1,2], C Bueno[1] and A Martínez-Serrano[1]

Understanding basic processes of human neural stem cell (hNSC) biology and differentiation is crucial for the development of cell replacement therapies. Bcl-X_L has been reported to enhance dopaminergic neuron generation from hNSCs and mouse embryonic stem cells. In this work, we wanted to study, at the cellular level, the effects that Bcl-X_L may exert on cell death during differentiation of hNSCs, and also on cell fate decisions and differentiation. To this end, we have used both v-myc immortalized (hNS1 cell line) and non-immortalized neurosphere cultures of hNSCs. In culture, using different experimental settings, we have consistently found that Bcl-X_L enhances neuron generation while precluding glia generation. These effects do not arise from a glia-to-neuron shift (changes in fate decisions taken by precursors) or by only cell death counteraction, but, rather, data point to Bcl-X_L increasing proliferation of neuronal progenitors, and inhibiting the differentiation of glial precursors. *In vivo*, after transplantation into the aged rat striatum, Bcl-X_L overexpressing hNS1 cells generated more neurons and less glia than the control ones, confirming the results obtained *in vitro*. These results indicate an action of Bcl-X_L modulating hNSCs differentiation, and may be thus important for the future development of cell therapy strategies for the diseased mammalian brain.
Cell Death and Differentiation (2007) **14,** 1880–1892; doi:10.1038/sj.cdd.4402205; published online 3 August 2007

The efficient generation of human neurons and glia from stem cells is the object of intense investigation, in the context of basic and preclinical cell replacement research.[1,2] Different means of genetic and epigenetic manipulations of stem cell cultures are being tested, aiming at enhancing their ability to generate the desired cell types.[3–6] In previous studies, we and others have demonstrated that Bcl-X_L overexpression has a major impact on the generation of dopaminergic neurons from human neural stem cells (hNSCs) and mouse embryonic stem cells (mES).[7,8] Also, recent data from conditional Bcl-X_L mutant mice add support to these observations.[9,10] In the present study, we are extending these observations and analyzing in detail the effects of Bcl-X_L on hNSCs differentiation, focusing on precursor cell fate choices, cell death, and precursor proliferation.

Bcl-X_L is the most potent antiapoptotic protein among Bcl-2 family members, both *in vitro* and *in vivo*.[11–14] More specifically, Bcl-X_L is essential for neuronal survival during brain development and in the adult central nervous system (CNS) (knockout mice and gene-expression studies[15,16]). In addition to its antiapoptotic role, recent studies have described new roles of Bcl-X_L in cell physiology – effects on Ca^{2+} homeostasis and gene expression[17] and synaptic transmission regulation[18] – under not necessarily apoptotic conditions. Several other studies have also described the role of Bcl-X_L in the control of cell cycle,[19,20] a process well known to be tightly linked to progression of precursor cells toward neuronal and glia differentiation.[21,22]

In this work, we aimed to elucidate the role of Bcl-X_L in the generation of neurons and glia from both v-myc immortalized and non-immortalized hNSCs.

In vivo, numerous studies have shown that hNSCs can integrate, migrate, and differentiate when transplanted into the developing or young adult rodent and primate brain.[1,2,23–25] Since neurodegenerative diseases are in many cases late-onset diseases, we found therefore of interest to study the *in vivo* properties of control or Bcl-X_L overexpressing hNS1 cells after transplantation into the aged rat brain. Consistent with the *in vitro* data, we have also observed an increased neuron production and a diminished glia yield from Bcl-X_L–overexpressing hNS1 cell transplants.

Results

Effects of Bcl-X_L on hNSCs differentiation. When studying the yield of β-III-tubulin$^+$ cells and GFAP$^+$ cells by control or stable Bcl-X_L hNS1 cells after 12 days of differentiation, we observed some interesting effects: (i) an increase in the percentage of neurons ($8.08 \pm 0.55\%$ in

[1]Department of Molecular Biology and Center of Molecular Biology 'Severo Ochoa', Autonomous University of Madrid-C.S.I.C. Campus Cantoblanco 28049, Madrid, Spain
*Corresponding author: I Liste, Department of Medical Biochemistry and Biophysics, Karolinska Institute, Scheelesväg 1, S-171 77 Stockholm, Sweden.
Tel: +46 8 52487620; Fax: +46 8 341960; E-mails: iliste@cbm.uam.es or Isabel.liste@ki.se
[2]These two authors contributed equally to this work.
Keywords: human neural stem cells; neurons; glia; aged brain; transplantation
Abbreviations: BrdU, bromodeoxyuridine; CNS, central nervous system; DAB, diaminobenzidine; Dcx, doublecortin; EGF, epidermal growth factor; FBS, fetal bovine serum; FGF2, basic fibroblast growth factor; GARPO, goat anti rabbit peroxidase; GFAP, glial fibrilary acid protein; GFP, green fluorescent protein; HAMPO, horse anti mouse peroxidase; hNSE, human neuron-specific enolase; hNSC, human neural stem cells; hNuc, human nuclei; ICC, immunocytochemistry; Map-2, microtubule-associated protein 2; mES, mouse embryonic stem cells; PI, propidium iodide
Received 13.9.06; revised 24.5.07; accepted 31.5.07; Edited by G Cossu; published online 03.8.07

control *versus* 21.87±0.87% for Bcl-X_L cells). (ii) A profound decrease in the percentage of glia (61.13±1.68% in control *versus* 12.88±0.85% in Bcl-X_L cells) (Figure 1a, b, d). (iii) The total number of cells per field was significantly increased in Bcl-X_L cultures (92±7.8 in control, *versus* 148±13 for Bcl-X_L cells) (Figure 1c, see also Figure 5c). And (iv) the percentage of differentiated cells (glia and neurons together) was decreased in the Bcl-X_L cultures (Figure 1e). As shown in Figure 1f, Bcl-X_L protein levels were increased in Bcl-X_L cells as compared to the controls, both under proliferation and differentiation conditions.

The data just described were obtained from a stable clone of hNSCs overexpressing Bcl-X_L for prolonged periods of time. To study Bcl-X_L effects in a shorter time scale, we infected control hNS1 cells with retroviral vectors coding for Bcl-X_L and green fluorescent protein (GFP), or only GFP (empty vector used as a control), on day 1 of differentiation, and the cells were let to differentiate until day 12. The efficiency of infection of both viral vector preparations was equivalent, as determined on day 3 post-infection (approximately 12–13% of GFP^+ cells; Supplementary Figure S1). Phenotypic analysis of GFP^+ cells after differentiation revealed that 70.3±1.4% of them in the Bcl-X_L group were β-III-tubulin$^+$, while only 20.5±1.8% were β-III-tubulin$^+$ in the control group ($P<0.01$; Student's *t*-test; $n=4$) (Figure 2a and b). On the contrary, the analysis of glial cell generation showed a significant reduction of GFP^+–$GFAP^+$ cells in Bcl-X_L transduced cells (14.4±1.3%) as compared with the empty vector group (34.4±0.9%) ($P<0.05$; Student's *t*-test; $n=4$) (Figure 2c and d).

To rule out the possibility that the observed Bcl-X_L effects could be related to an interaction of Bcl-X_L with v-myc in the cellular context, we studied the effects of Bcl-X_L on the differentiation of non-immortalized forebrain hNSCs. Cells were infected with the same vectors as described above, and their differentiation was studied. Efficiency of infection was in the range of 9–12%, similar to that seen in immortalized cells. As shown in Figure 2e–g, Bcl-X_L overexpression resulted in a higher yield of neurons, and a parallel decrease in the number of $GFAP^+$ cells generated.

Therefore, the Bcl-X_L effects described so far are not related to a prolonged exposure of the cells to high Bcl-X_L levels, neither to v-myc nor the nature of the hNSCs (either cell lines or non-immortalized cultures).

Differentiation 'time course' of control or stable Bcl-X_L overexpressing hNS1 cells. To obtain further insights into Bcl-X_L effects, we studied the time course of differentiation of both control and Bcl-X_L hNS1 cells. Neurons (β-III-tubulin$^+$ cells) were generated at the same pace by both cell types.

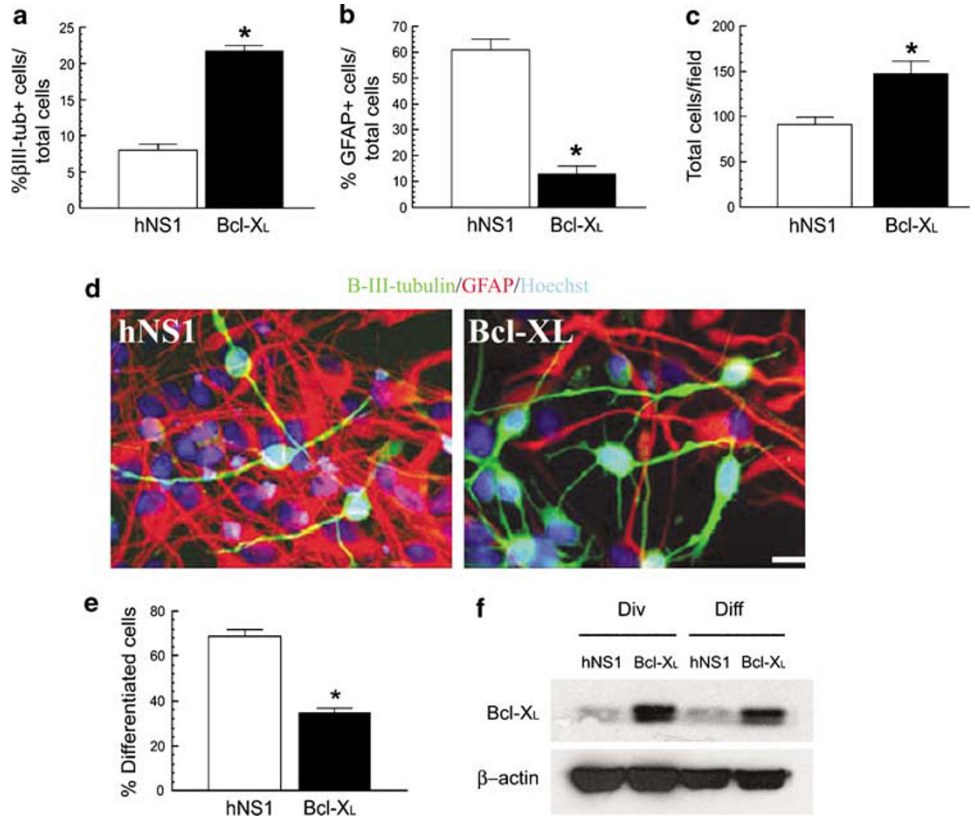

Figure 1 Bcl-X_L effects on glia and neuron generation by hNS1 cells. Control or Bcl-X_L overexpressing hNS1 cells were differentiated for 12 days. (**a** and **b**) Percentage of β-III-tubulin$^+$ and $GFAP^+$ cells. (**c**) Total cells per field examined (eight fields in each of five individual experiments), and (**d**) ICC for β-III-tubulin$^+$ and $GFAP^+$ cells. Scale bar, 20 μm. (**e**) Percentage of differentiated cells (β-III-tubulin$^+$ or $GFAP^+$) in control or Bcl-X_L cells. Data represent means±S.E.M. ($n=5$ from one experiment; results confirmed in three independent experiments) (*$P<0.05$, statistically significant difference between control and Bcl-X_L groups, Student's *t*-test). (**f**) Western blot of control or Bcl-X_L–hNS1 cells under division (Div) or differentiation (Diff) conditions; blots were double-stained for Bcl-X_L and β-actin, as a loading control

The neuronal yield was higher in Bcl-X_L cultures at every time-point studied (Figure 3a and c). Glial cells (GFAP$^+$) appeared on the same days for both types of cultures, but their numbers were significantly less in Bcl-X_L cultures than in control cells (Figure 3d and f). Normalized data for neurons (Figure 3b) and glia (Figure 3e) indicated that GFAP

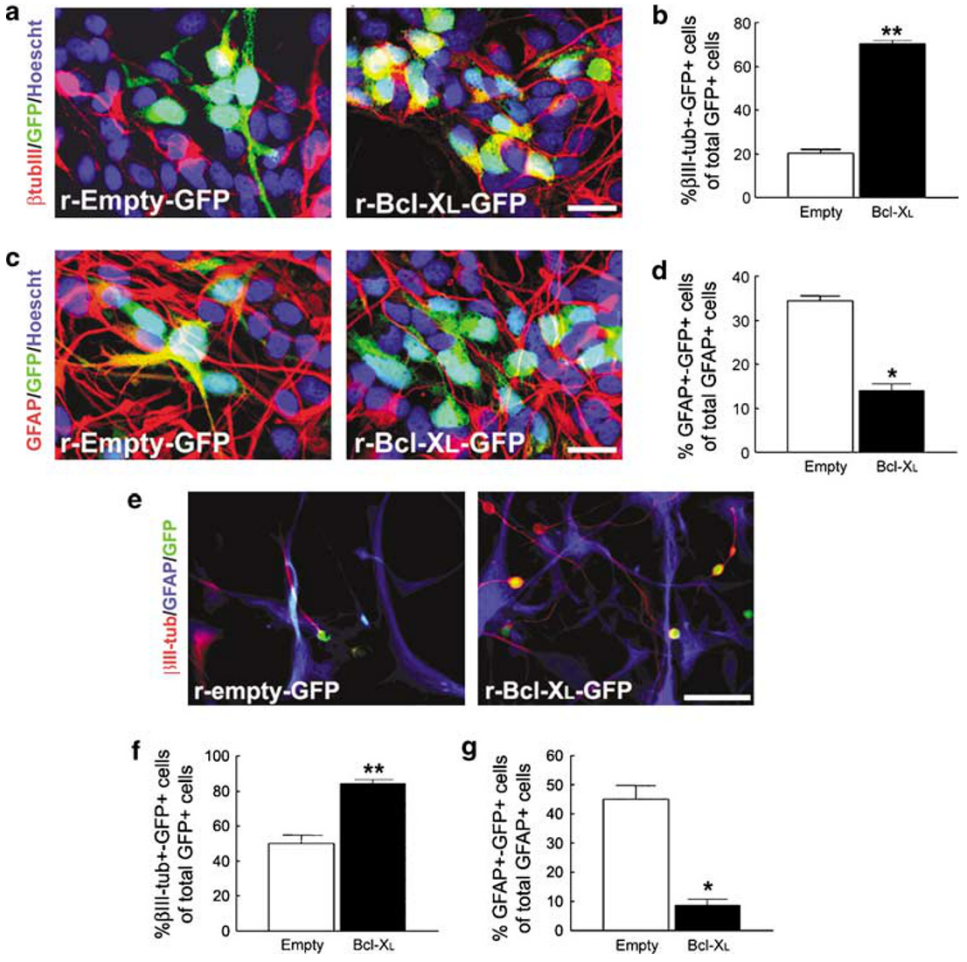

Figure 2 Retroviral transduction of hNSCs for Bcl-X_L expression. (**a**–**d**) Bcl-X_L overexpression increases neurogenesis and diminishes gliogenesis from hNSCs. hNS1 cells were transduced with retroviral vectors on day 1 of differentiation, and analyzed on day 12. *$P<0.05$; **$P<0.01$, Student's *t*-test; $n=4$. More than 1000 GFP$^+$ cells (approximately 300 cells per well) per group were analyzed. Scale bar in (**a** and **c**), 20 μm. (**e**–**g**) hNSCs (forebrain, non-immortalized neurosphere cells) were transduced with the same retroviral vectors as above. (**e**) Representative IF photographs of the transduced cultures. Scale bar, 20 μm. As shown in panels (**f** and **g**) the yield of neurons among GFP$^+$ cells was increased by two-fold in Bcl-X_L overexpressing cells. Conversely, GFAP$^+$ cells generation was diminished by approximately 70–80%, after Bcl-X_L overexpression. (Data represent means $\pm$ S.E.M from four independent experiments, approximately 100 GFP$^+$ cells were analyzed per experiment on day 7 of differentiation. *$P<0.05$ and **$P<0.01$; Student's *t*-test)

Figure 3 Time course of neuron and glia generation by control and Bcl-X_L hNS1 cells. The percentage of β-III-tubulin$^+$ and GFAP$^+$ cells on diverse differentiation days are shown in panels (**a** and **d**), respectively. Cells were seeded at a density of 40 000 cells/cm^2. Data represent means $\pm$ S.E.M ($n=5$). Asterisks indicate a statistical difference between control and Bcl-X_L cells on the indicated days (*$P<0.05$; **$P<0.01$; two-way ANOVA followed by *post hoc* Student's *t*-test). (**b** and **e**) These panels illustrate the comparative rate of neuron and glia generation for each cell type, after normalization of the data shown in (**a** and **d**) (a 100% value was assigned to the maximum absolute value in (**a** and **d**)). Note that the temporal profile for neuron generation is absolutely parallel for control and Bcl-X_L cells. Also, that there can be a slight delay in the appearance of GFAP$^+$ cells on days 3–7. (**c** and **f**): The differentiation time-course experiment shown in (**a** and **d**), was re-done to cover longer time points (days 12–21), to elucidate if there could be a delay in differentiation of glia. To avoid cell overconfluence related problems in this new experiment running over 3 weeks, cells were plated at a lower cell density (20 000 cells/cm^2). Analysis of the results (two-way ANOVA) failed to detect any time differences on day 12 and after in each group, neither for the case of glia nor for neurons, ($P>0.05$ in both cases). The asterisks in (**c** and **f**) indicate a statistical significant difference between control and Bcl-X_L cells (two-way ANOVA, followed by *post hoc* Student's *t*-test; *$P<0.05$, **$P<0.01$). Last, cell density does not play any role in Bcl-X_L effects reported in these experiments (comparison of data on day 12 in panels (**a** and **d**) to those of (**c** and **f**), Student's *t*-test; $P>0.1$). The percentages of Map-2$^+$ and synapsin-I$^+$ cells are represented in (**g** and **h**), respectively. Both graphs show a similar profile to that observed in the β-III-tubulin$^+$ cells graph, thus not detecting an early appearance of a mature phenotype in overexpressing Bcl-X_L cells compared to hNS1 cells. In the Map-2 data, there are statistical differences between the two cell types (two-way ANOVA, cellular effect $F_{(6,37)}=15.5235$, $P=0.0003$) but not in the synapsin-I data (two-way ANOVA, cellular effect $F_{6,37}=0.754516$, $P=0.39$). Double immunostaining for Map-2 and synapsin-I in control and Bcl-X_L cells is shown in (**i**). The graphs represent the percentage of vimentin$^+$ (**j**) and vimentin$^+$–GFAP$^+$ cells (**k**) along the differentiation period; no statistical differences are detected for vimentin$^+$ cells between the two cell types (two-way ANOVA, cellular effect, $F_{(1,35)}=0.49495$, $P=0.4864$), when studying the appearance of double vimentin$^+$–GFAP$^+$ cells, there are statistical differences (two-way ANOVA, cellular effect; $F_{(6,42)}=156.948$, $P<=0.0001$). A representative picture of double immunostaining for vimentin and GFAP is shown in (**l**). Scale bar 20 μm for (**i** and **l**)

generation might be delayed in Bcl-X_L cells. To rule out this possibility, we conducted an additional series of experiments aimed to reach day 21 of differentiation (Figure 3c and f). As a result, we got the same information as shown before in panels a and d, even when prolonging the time of differentiation. To strengthen the data obtained above, we performed the same time course and assay cell cultures for microtubule-associated protein 2 (Map-2) and synapsin-I markers, which both show the same pattern as β-III-tubulin$^+$ cells, confirming our previous conclusions (Figure 3g–i).

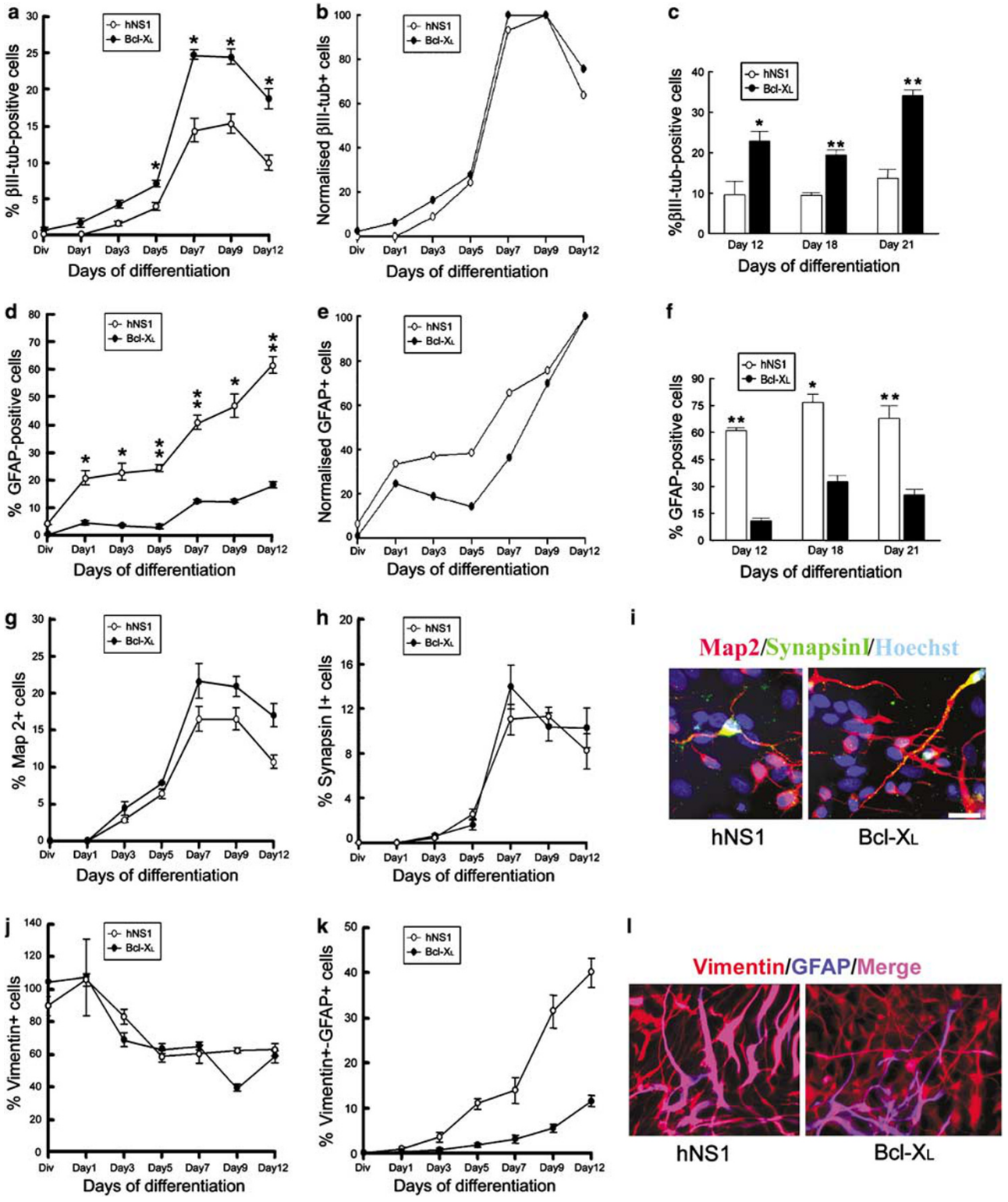

Regarding glia cells, we quantified the vimentin$^+$ cells and observed that their number decreased in the same amount for Bcl-X_L and control cultures (Figure 3j). Moreover, the vimentin cells start to express GFAP along the time of differentiation; quantification of the vimentin$^+$-GFAP$^+$ cells appearing in the culture (Figure 3k and l) showed that this number was greatly decreased in Bcl-X_L cultures, as compared to the controls. These data suggest that the transition between vimentin$^+$ cells to mature glia (GFAP$^+$) is prevented by Bcl-X_L in hNS1 cultures.

Cell death during differentiation. To ascertain the role of cell death during differentiation of hNS1 cells, we studied several cell death-related parameters (Figure 4): (i) number of alive/dead–dying cells (calcein/PI staining of alive cultures, Figure 4a); (ii) percentage of cells with fragmented DNA determined by flow cytometry (cells fitting in the sub-G_0/G_1 region of the nuclear DNA distribution) which indicates programmed cell death, Figure 4b); (iii) number of cells showing a condensed/fragmented nucleus (Hoechst staining microscopy, Figure 4c); (iv) the percentage of Annexin-V$^+$ cells (cells undergoing a programmed cell death process, Figure 4d). Data obtained with all four techniques illustrate that cell death is not a major event taking place in our system during the differentiation 'time course'. The proportion of alive and dead–dying cells did not substantially change with time.

To obtain further insights, we assessed the undergoing apoptosis for every phenotype along the differentiation period. We quantified the number of cells co-labeled for cleaved caspase-3 and β-III-tubulin, GFAP and nestin, respectively (Figure 4e–g). As shown in Figure 4e and f, Bcl-X_L protects the neurons and neural cells against cell death as compared to controls, but at very low rate (less than 2%). Moreover, we have not found any double caspase-3$^+$-GFAP$^+$ cells.

Bcl-X_L effects on cell proliferation during the differentiation period. To investigate Bcl-X_L effects on cell proliferation, we first performed a pulse and chase experiment (Figure 5a). Using this experimental design, we detected a trend for an increase in the number of cells incorporating bromodeoxyuridine (BrdU) in Bcl-X_L cultures as compared with control hNS1 cells on days 3–5 of differentiation (Figure 5b and e). Consistent with this, the total number of cells in the Bcl-X_L cultures increased from day 5 onwards in comparison to control cultures (Figure 5c).

To have a second confirmation of the presence of proliferating cells in the cultures, we stained parallel samples for Ki-67 (a marker expressed during most of the cell cycle[26]) and, as expected, we found more cells still in cycle in Bcl-X_L cultures, from day 5 onwards (Figure 5d and e).

Bcl-X_L modulates the production of neurons and glia from their precursors. Since cell death or differences on the time set of neurons and glia production were not the decisive cause of different yielding observed; and because existence of a trend on an increased proliferation in Bcl-X_L cultures detailed above, we investigated what precursors of both cell types render on after the differentiation. With this aim, we pulsed the cells on different days and allowed them to differentiate until day 12 (Figure 6a). As Figure 6b and c show, there are higher number of cells that, when pulsed in the first days of differentiation, produce more neurons, detected as double β-III-tubulin$^+$–BrdU$^+$ in Bcl-X_L cultures. However, the opposite happens for GFAP$^+$ cells (Figure 6c and d), there are less GFAP$^+$–BrdU$^+$ in Bcl-X_L overexpressing cells. We concluded that Bcl-X_L is increasing the number of precursor proliferation that render on β-III-tubulin cells on day 12 or that these precursors differentiate more in Bcl-X_L cultures, it means an induction of the neuron phenotype. In the case of GFAP cells, it is a matter of decreased precursor proliferation or a hampered differentiation.

Bcl-X_L promotes the proliferation of neural (Nestin$^+$) and neuronal precursor (β-III-tubulin$^+$) cells at early times during differentiation of hNS1 cells but not of vimentin$^+$ cells. In order to discern between the two possibilities raised on the above experiment, we analyzed the immediate phenotype of the proliferating cells during the differentiation period and studied Bcl-X_L effects on them. We pulsed differentiating cell cultures for 24 h with BrdU (Figure 7a), and the cells were subsequently processed for immunocytochemistry (ICC) (Figure 7b).

Quantification of BrdU- or Nestin$^+$ cells revealed a similar temporal profile for both markers over the studied time course (Figure 7c and d). Bcl-X_L increased the number of BrdU$^+$ and Nestin$^+$ cells during the whole of the differentiation period, as compared to the controls. Quantification of the number of double BrdU$^+$–Nestin$^+$ cells (Figure 7e) indicated that most of the BrdU$^+$ cells were Nestin$^+$, while approximately one half of the Nestin$^+$ cells incorporated BrdU. This was expected, considering that the hNS1 cells have a cell-cycle length of 40 h[27,28] and that they were exposed to BrdU for 24 h only. Bcl-X_L did not influence these figures substantially, but at days 3–4 of differentiation, a two-fold increase in the number of Nestin$^+$ cells also incorporating BrdU was detected. Overall, Ki-67, Nestin, and BrdU data (Figures 5 and 7b–e) suggest that Bcl-X_L is promoting cell proliferation.

Figure 4 Cell death during differentiation of hNS1 cells. Four different experimental approaches were explored: (**a**) Vital stains using calcein-AM and PI. (**b**) Determination of the number of cells fitting in the sub-G_0/G_1 region of nuclear DNA distribution (dead–dying cells) by flow cytometry. (**c**) Nuclear morphology using Hoechst 33258, to determine the number of cells showing a damaged nucleus (showing condensed chromatin and/or nucleus fragmentation). (**d**) Annexin-V ICC, showing cells undergoing programmed cell death. In conclusion, cell death does not play a major role in these experiments (Asterisks indicate $^*P<0.05$, $^{**}P<0.01$, two-way ANOVA followed by *post hoc* Student's *t*-test). (**e** and **f**) Percentages of the number of cells co-labeled for cleaved caspase-3 and Nestin (related to total Nestin$^+$ cells) or β-III-tubulin (related to total β-III-tubulin$^+$ cells) along the differentiation period in control hNS1 or Bcl-X_L overexpressing hNS1 cells. In both cases, there are statistical differences (two-way ANOVA, cellular effect $F_{(6,37)}=87.8645$, $P<0.0001$; two-way ANOVA, cellular effect $F_{(6,37)}=14.5973$, $P=0.0007$, respectively). Representative pictures of double immunostaining for caspase-3 (green) and Nestin, β-III-tubulin (arrow heads) or GFAP (red) in control or Bcl-X_L cells are shown in (**g**). Colocalization between caspase-3 and GFAP was never observed. Nuclei are counterstained in blue by Hoechst

Next, we analyzed the extent of GFAP or β-III-tubulin precursor cells that were proliferating at the time points analyzed, and if Bcl-X_L had any effect on their proliferation.

As shown in Figure 7f, the percentage of total cells staining for GFAP and BrdU was almost negligible during the time course (below 1% of the total number of cells). Furthermore,

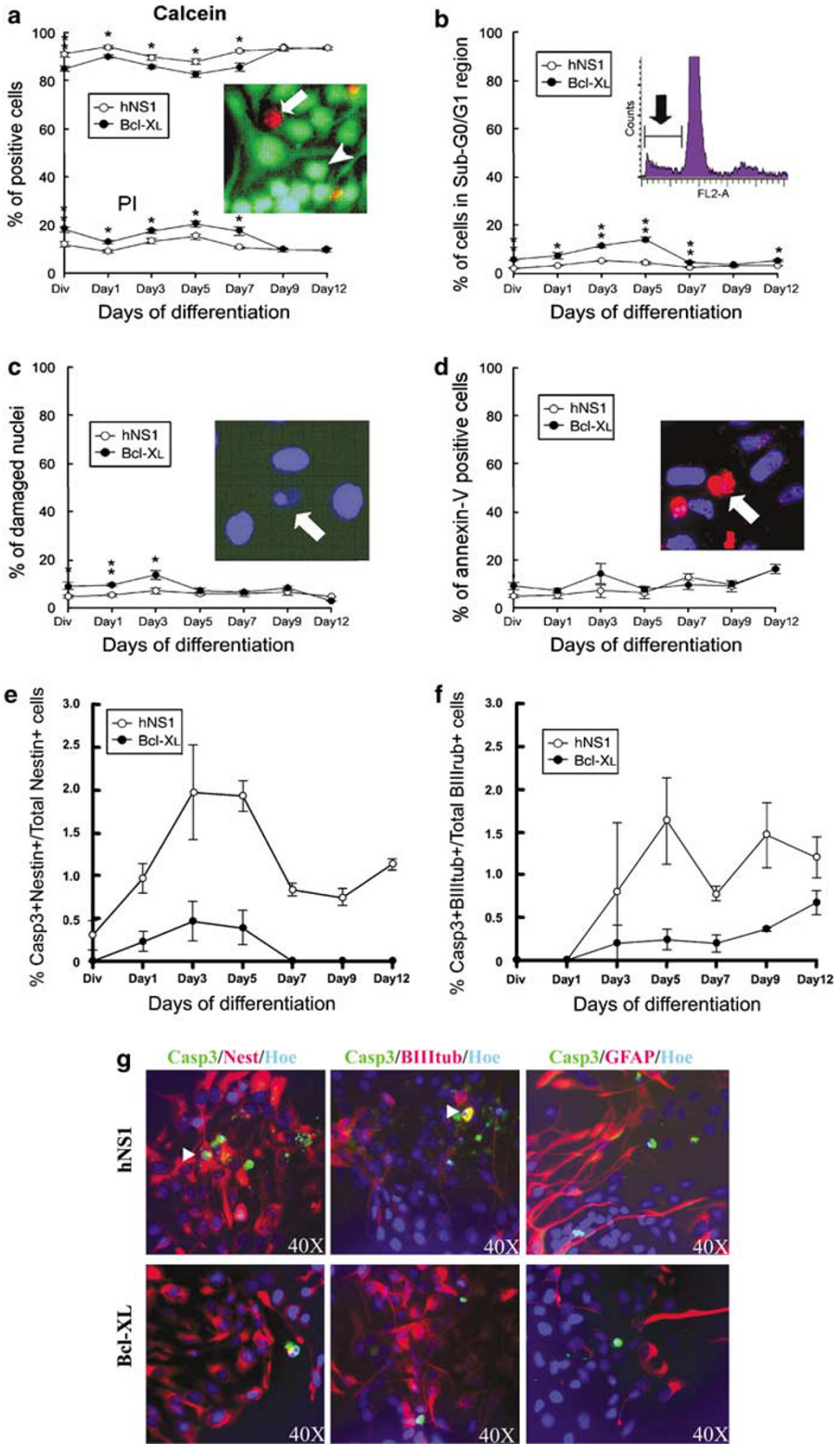

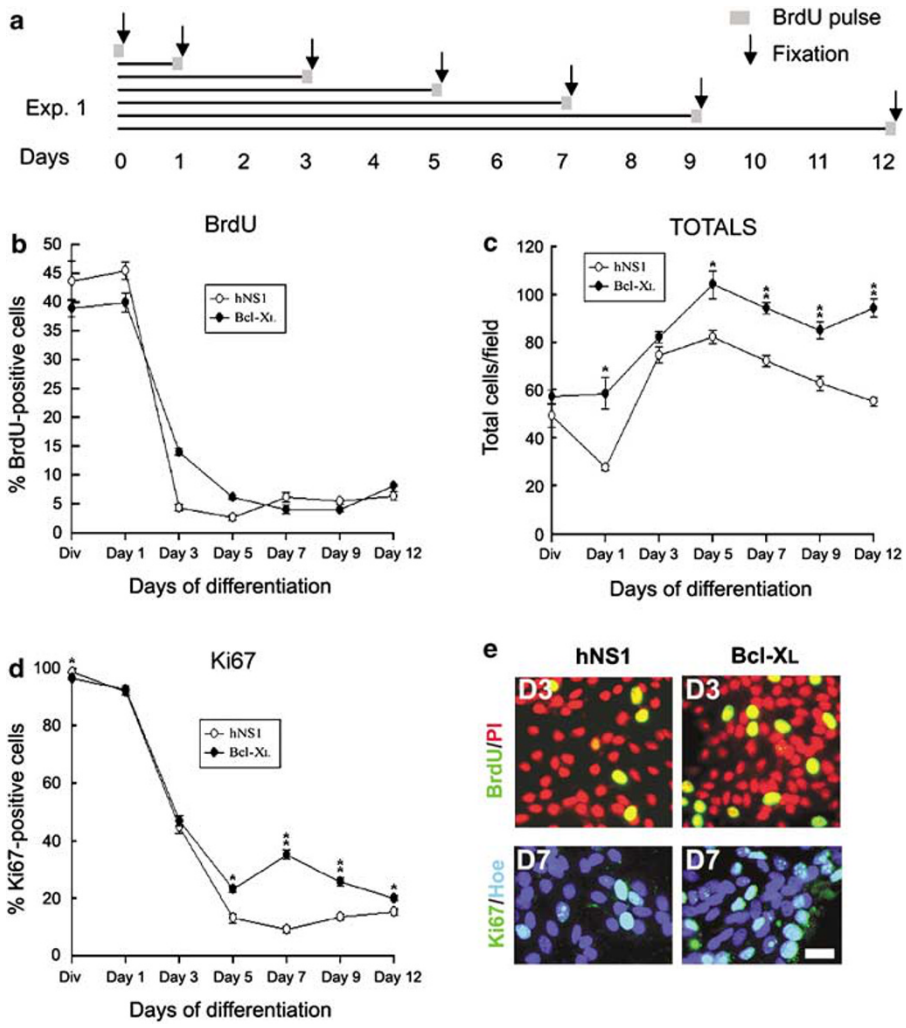

Figure 5 Cell proliferation during differentiation of control and Bcl-X_L hNS1 cells. (**a**) Schematic representation of the BrdU pulse performed in this experiment (Experiment 1 in Materials and Methods section). The cells were incubated with 10 μM BrdU during 2 h on days 0, 1, 3, 5, 7, 9, 12 of differentiation, and immediately fixed afterwards (arrows). Percentage of cells incorporating BrdU after BrdU pulse and total cell numbers during differentiation are represented in **b** and **c**, respectively. (**d**) Percentage of cycling cells (Ki-67$^+$) along the differentiation period. Data represent means $\pm$ S.E.M. ($n=4$). Asterisks indicate a statistical difference between control and Bcl-X_L hNS1 cells (*$P<0.05$; **$P<0.01$; two-way ANOVA, followed by a *post hoc* Student's *t*-test). (**e**) BrdU/PI and Ki-67/Hoechst stainings are shown at the most relevant days (3 and 7 days, respectively), during the differentiation period. Scale bar, 20 μm

it did not significantly change with time, or after Bcl-X_L overexpression. Owing to this result, we checked the percentage of vimentin$^+$–BrdU$^+$ cells and observed that Bcl-X_L overexpression does not have any effect on vimentin$^+$ cell proliferation (Figure 7h).

In the case of β-III-tubulin$^+$ cells (Figure 7g), Bcl-X_L cultures showed an increase of β-III-tubulin$^+$–BrdU$^+$ cells, particularly during the early days of the time course, while control hNS1 cells did only show a very low percentage of these cells being positive for BrdU and β-III-tubulin (around 1% in control cultures). All of these data indicated an increase of proliferating Nestin$^+$ cells, neuron progenitor proliferation and non-influence on glia lineage proliferation. Moreover, the proportion of β-III-tubulin$^+$–BrdU$^+$ cells to total β-III-tubulin$^+$ pool is the same for Bcl-X_L cultures as control one, while the proportion of β-III-tubulin$^+$-BrdU$^+$ cells to the total mitotic (BrdU$^+$) cells is higher in Bcl-X_L overexpressing cells, corroborating the data explained above (Supplementary Figure S2).

Bcl-X_L effects on hNS1 cell grafts into the aged rat striatum. Four weeks after intrastriatal cell implantation, three out of five rats receiving control cells, or four out of five animals implanted with Bcl-X_L hNS1 cells had surviving grafts, as determined by the presence of human nuclei (hNuc) stained cells (Figure 8a). hNuc$^+$ cells were mainly located at the striatal implantation site and no signs of tumor formation were observed in any transplanted animals, according to previous studies.[8,29,30] Morphometric assessment of graft properties indicated that graft volume was larger for Bcl-X_L cell grafts as compared to control cell grafts. (i) Antero-posterior extension of the grafts was 0.53 ± 0.13 mm in control grafts and 1.09 ± 0.11 mm in Bcl-X_L transplants ($P<0.05$; Student's *t*-test). (ii) Total graft

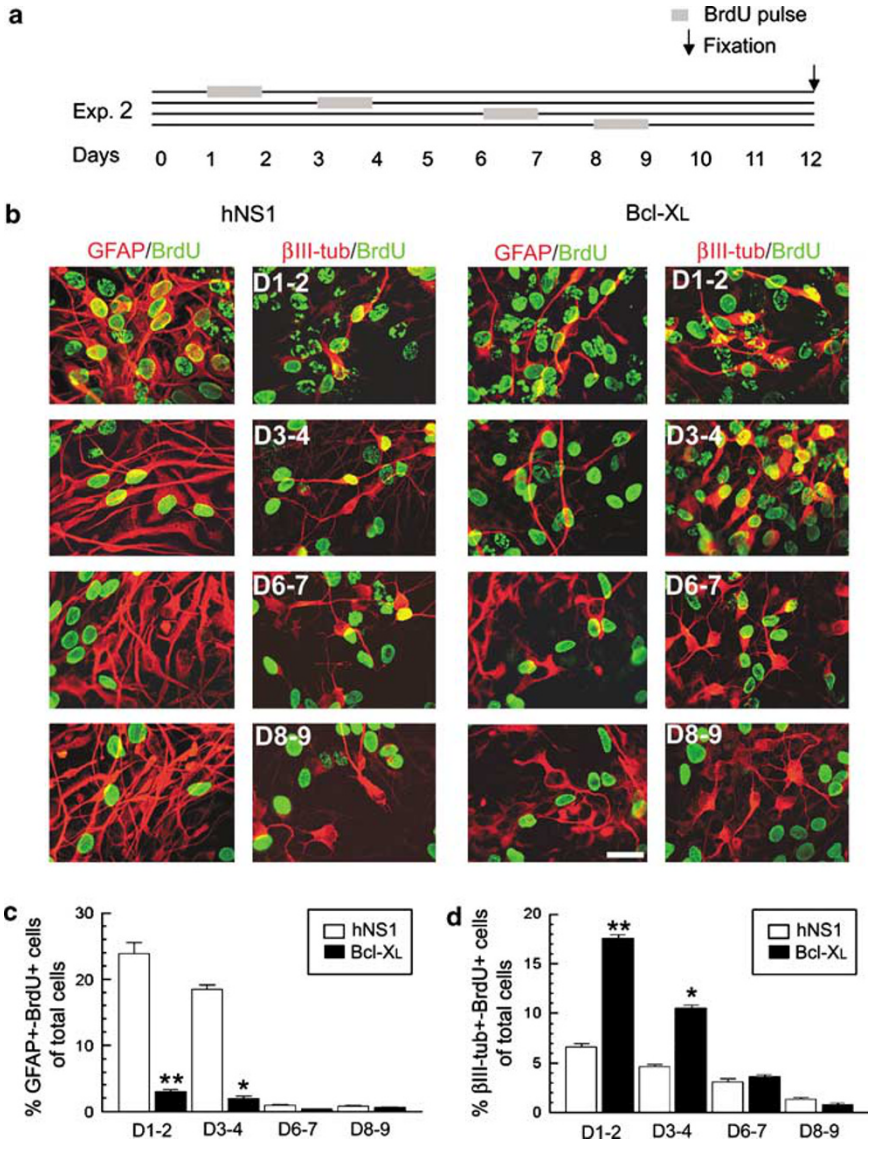

Figure 6 Birth dating of neurons and glia. (**a**) In this experiment (Experiment 2 in Materials and Methods section), hNS1 cells were pulsed with BrdU (1 μM) for 24 h at the indicated times and let to differentiate until day 12, being subsequently fixed (arrow). (**b**) Double IF for GFAP or β-III-tubulin, and BrdU, in control or Bcl-X_L overexpressing hNS1 cells. The histograms in (**c** and **d**) show the percentage of cells being GFAP$^+$-and-BrdU$^+$ or β-III-tubulin$^+$-and-BrdU$^+$ related to the total number of cells present in the cultures, respectively. Data represent means$\pm$S.E.M. ($n=4$). Asterisks indicate a statistical difference between control and Bcl-X_L hNS1 cells. (*$P<0.05$; **$P<0.01$, two-way ANOVA, followed by *post hoc* Student's *t*-test)

volume increased from $0.032\pm0.006\,mm^3$ in control cell grafts to $0.34\pm0.05\,mm^3$ in Bcl-X_L grafts ($P<0.05$; Student's *t*-test). In agreement with previous results obtained in grafting studies in neonatal or young adult rats,[8,29,30] control hNS1 cells generated very few doublecortin (Dcx$^+$) or human neuron-specific enolase (hNSE$^+$) neurons when grafted into the striatum of aged rats, as expected from a non-neurogenic area, and aged tissue environment, receiving a NSCs graft. In contrast, Bcl-X_L cell transplants were richer in Dcx$^+$ and hNSE$^+$ cells, as obvious from graft examination. Quantification of cell numbers was precluded by the high cell density of the grafted cells. Grafts of control hNS1 cells showed a dense (intense) GFAP immunoreactivity, sending an extensive network of processes to the host brain. GFAP immunoreactivity was also present in Bcl-X_L grafts, but this was less intense and more confined to the transplant site.

Phenotypical identities of the grafted cells were analyzed by double labeling for hNuc$^+$ and Nestin$^+$ (undifferentiated precursors), Dcx$^+$ (neuroblasts) or GFAP$^+$ (glia), under confocal *z* axis serial images (Figure 8b). No hNuc$^+$–Nestin$^+$ or hNuc$^+$–Dcx$^+$ cells were detected in the striatal grafts of control hNS1 cells, in contrast with the abundance of double-labeled cells found for both antigens in the Bcl-X_L grafts ($22.13\pm2.6\%$ of hNuc$^+$–Dcx$^+$ and $26.1\pm1.3\%$ of hNuc$^+$–Nestin$^+$ cells, respectively; mean$\pm$S.E.M.). Conversely, many hNuc$^+$–GFAP$^+$ cells were found in control grafts ($96.2\pm0.85\%$) whereas in the Bcl-X_L grafts their number was markedly reduced ($24.6\pm4.3\%$) ($P<0.01$; Student's *t*-test).

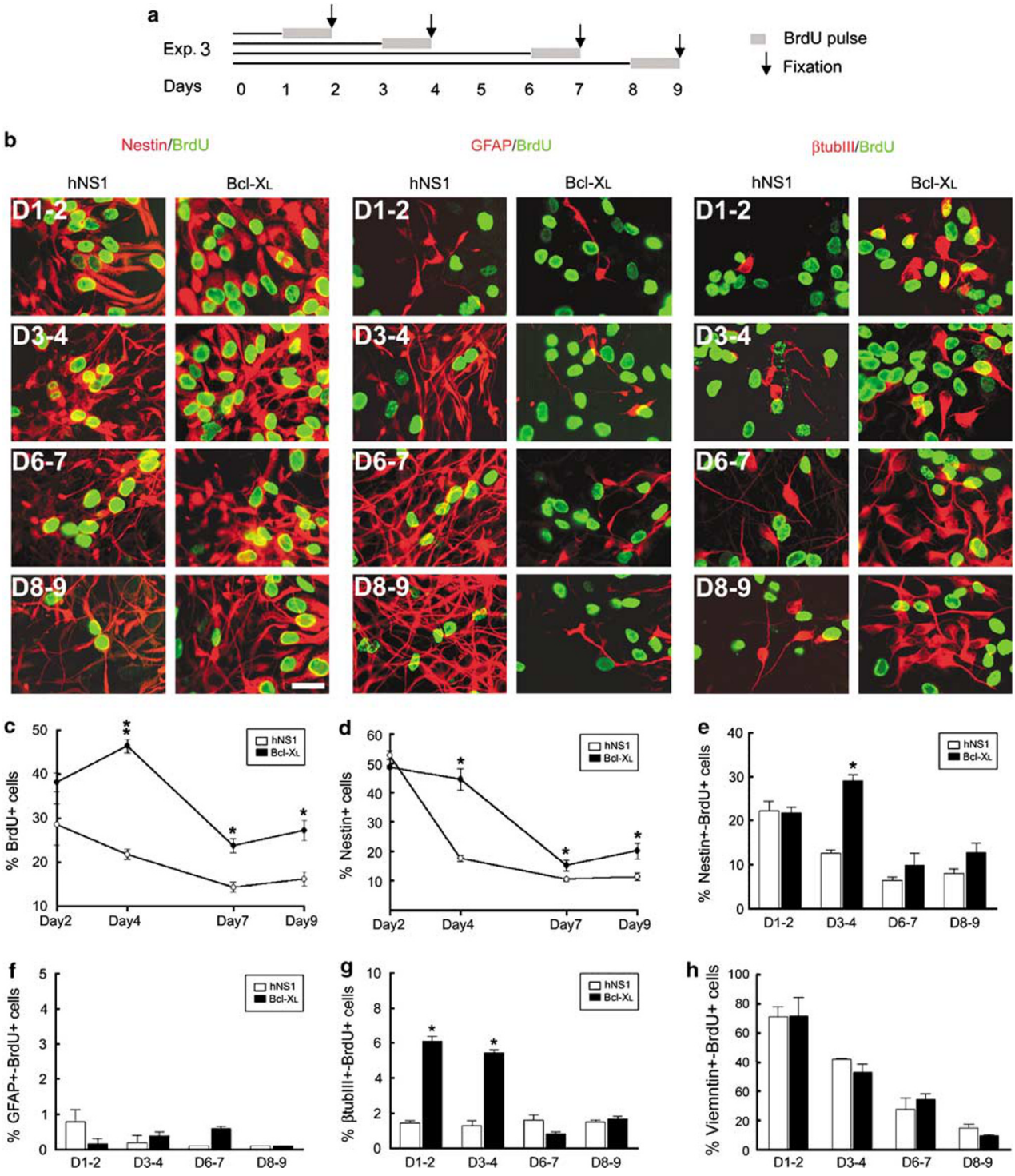

Figure 7 Double immunolabeled cells for BrdU and: Nestin, GFAP, β-III-tubulin, or vimentin during differentiation of hNS1 cells. Effects of Bcl-X_L. (**a**) Schematic representation of the BrdU pulse performed in this experiment (Experiment 3 in Materials and Methods section). The cells were incubated with 1 μM BrdU during 24 h on days 1, 3, 6, and 8 of differentiation, and fixed afterwards (arrows). (**b**) Double IF for Nestin, GFAP, or β-III-tubulin combined with BrdU in control or Bcl-X_L overexpressing hNS1 cells. Scale bar, 20 μm. (**c**–**e**) Percentages of BrdU and Nestin$^+$ cells, and the percentage of Nestin$^+$ ones from the total number of proliferating cells (BrdU$^+$). Note the similar temporal profiles for BrdU incorporation and Nestin expression. (**f**–**h**) Percentages of GFAP$^+$, β-III-tubulin$^+$, or vimentin$^+$ cells (relative to the total number of cells) that incorporated BrdU on the indicated days. Asterisks indicate a statistical difference between control and Bcl-X_L cells. (*$P<0.05$, **$P<0.01$; two-way ANOVA followed by a *post hoc* Student's *t*-test)

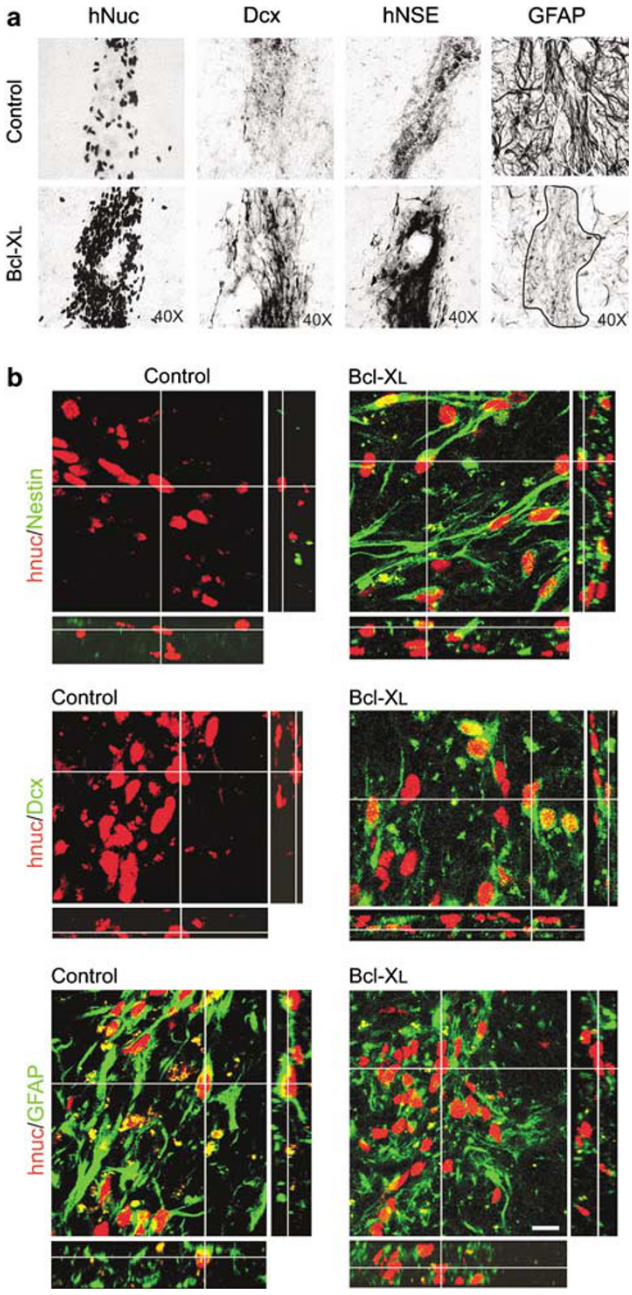

Figure 8 Bcl-X_L effects on hNS1 cell transplants. (**a**) DAB immunostaining for hNuc, Dcx, human neuron-specific enolase (hNSE), or GFAP in serial sections from animals (aged rats, 23 months of age) receiving intrastriatal transplants of control or Bcl-X_L overexpressing hNSCs. Note the abundance of cells immunereactive for hNuc, Dcx, and hNSE in the Bcl-X_L grafts as compared with control cell grafts, and the decrease in GFAP$^+$ cells. Magnification was 40 $\times$ in all cases. (**b**) Z-stack confocal images of double IF stains for hNuc and Nestin, Dcx, or GFAP from control or Bcl-X_L-overexpressing hNS1 cells grafted into the aged striatum. Numerous hNuc$^+$/Dcx$^+$ cells and hNuc$^+$/Nestin$^+$ cells were found in Bcl-X_L cell grafts, which were absent in control cell grafts. Conversely, many GFAP$^+$ cells were identified as human cells (hNuc$^+$) in control cell grafts, but their number was dramatically decreased in Bcl-X_L hNSCs grafts. Scale bar, 10 μm

Discussion

Understanding how human stem cells can generate differentiated neural cell types is crucial for basic developmental studies and for the development of future cell therapies for nervous system diseases.[1,2] Our data indicate that transient Bcl-X_L overexpression instructively direct the fate of both immortalized and naive hNSCs towards neurons while decreasing glia generation. These effects were even more prominent in stable Bcl-X_L-overexpressing immortalized hNSCs, and they could be related to the following.

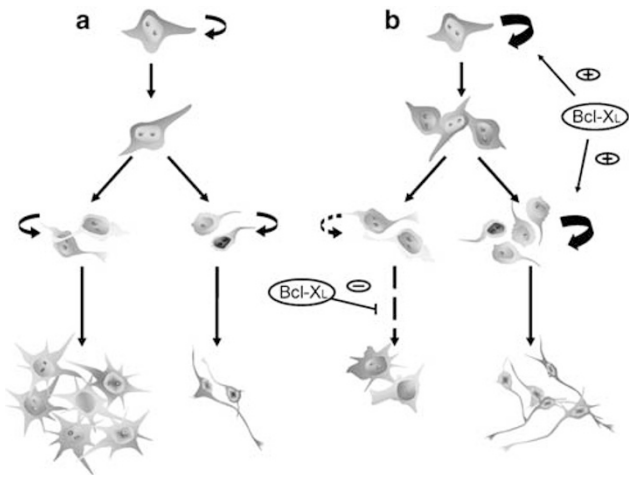

Figure 9 Model for Bcl-X_L effects on hNS1 cells, *in vitro*. (**a**) Proposed scheme of differentiation of control and (**b**), of Bcl-X_L overexpressing hNS1 cells. All data shown here consistently demonstrate that Bcl-X_L enhances neuroblast proliferation and decreases the differentiation of glia, at the same time. It is important to note that mitotic precursors for glial cells do not express GFAP while being proliferative cells, while neuronal mitotic precursors (neuroblasts) stain positive for β-III-tubulin at very early stages. Bcl-X_L does not alter the timing of differentiation of hNS1 cells. As demonstrated in the experiment shown in Figure 7, Bcl-X_L may stimulate the division of Nestin$^+$ cells

Survival. The antiapoptotic role of Bcl-X_L has been well established in previous studies dealing with the differentiation of neural progenitors, and neural cells, in general.[9,13,14] Bcl-X_L is required for neuronal survival during brain development and in the postnatal period.[16] Indeed, extensive apoptotic cell death was observed in the developing brain of Bcl-X_L-deficient mice embryos.[15] Bcl-X_L has also been recently reported to play a crucial role in neuronal development/survival in conditional null mice specific for catecholaminergic cells.[9] Our data indicated that total cell death is not playing a major role in our differentiation system neither in absolute terms, nor with time. However, and according to other studies, a decrease in apoptotic (caspase-3$^+$) cell death of Nestin$^+$ and β-III-tubulin$^+$ cells was observed in stable Bcl-X_L overexpressing cells as compared to control hNS1 cells along the differentiation period. This antiapoptotic effect, even not irrelevant, seems to be too small to explain *per se* the high increase of in *vitro* generated neurons and the dramatic reduction in the yield of glial cells in Bcl-X_L cultures, but we do not discard a minor protective effect in neural and neuronal cells.

Differentiation. When the β-III-tubulin and GFAP generation time courses are studied in detail, we conclude that Bcl-X_L effects were due to the magnitude, not the rate, of neurons and glia generation. This observation was reinforced by the study of more mature neuronal markers (Map-2 and

synapsin-I), which showed similar profiles of expression over time. Turning to glia, we also performed a time course to study vimentin cells, which decreased at the same pace for both cell types (control or Bcl-X_L).

Similar results, in terms of neuron/glia generation were observed when cells were run until day 21 of differentiation, therefore discarding a possible 'delay of differentiation'.

Progenitor proliferation during hNS1 cell differentiation. BrdU incorporation data showed a trend for an increase in the number of $BrdU^+$ cells in Bcl-X_L cells as compared to control cultures on day 3 of differentiation. The percentages of Ki-67^+ cells, and total cell numbers were also significantly increased in Bcl-X_L cultures after day 5 of differentiation. These results strongly indicate that Bcl-X_L is modulating – cell proliferation in our system, in agreement with other reports.[19,20]

The analysis of the proliferation of neural precursor cells ($Nestin^+$–$BrdU^+$), glia progenitor/precursor cells ($GFAP^+$–$BrdU^+$ and $vimentin^+$–$BrdU^+$), and neuronal progenitors (β-$III\text{-}tubulin^+$–$BrdU^+$) showed: Firstly, the quantification of $BrdU^+$ or $Nestin^+$ cells confirmed the expected parallel temporal profile for both markers and Bcl-X_L increased the numbers of stained cells during the whole of the differentiation period. These findings are consistent with results from studies using mES cells,[7] and *bax–bak*-deficient mice which displayed an increased pool of progenitor cells in the subventricular zone.[31] Second, quantification of double $BrdU^+$–$Nestin^+$ cells indicated that most of the proliferating cells ($BrdU^+$) were $Nestin^+$, while approximately one half of the $Nestin^+$ cells incorporated BrdU. Moreover, Bcl-X_L overexpression increased twofold the number $BrdU^+$–$Nestin^+$ cells pulsed during days 3–4. These data suggest that Bcl-X_L is promoting the proliferation of undifferentiated ($Nestin^+$) cells (see Figure 9).

Third, BrdU incorporation into $GFAP^+$ precursor cells was negligible, and Bcl-X_L had no effect on this parameter. We performed the same BrdU marking strategy with vimentin cells and observed that they incorporated BrdU at the same rate even when Bcl-X_L was overexpressed, allowing us to state that Bcl-X_L does not affect the proliferation of immature glia. Finally, the number of neuronal precursor cells incorporating BrdU (β-$III\text{-}tubulin^+$–$BrdU^+$ cells) was increased in Bcl-X_L cultures. Overall, we concluded that Bcl-X_L promotes the proliferation of neural precursors and neuronal progenitors, that the last phenomenon may be responsible for the increased number of post-mitotic neurons, and that the diminished production of glia is due to a block in differentiation of their precursors.

Regarding the mechanism explaining the increase in neuron generation observed here after Bcl-X_L overexpression, it is important to highlight that cell proliferation has been shown to be a prerequisite for increased neuron generation in other studies.[22] Present results could be reminiscent to those observed after valproate (an inhibitor of histone deacetylase) treatment of human fetal forebrain stem cells.[5] Similarly, Wnts have been recently found to enhance neurogenesis from hippocampus-derived precursors, through the stimulation of neuroblast proliferation.[6] Also, pro-neural transcription factors of the helix–loop–helix family, such as neurogenin and Mash1[32,33] have been reported to enhance neuron generation through an increased proliferation of their progenitors. In fact, Mash1 deletion mutant mice show decreased cell proliferation, and reduced brain size and neuronal generation/differentiation in the ventral forebrain.[34] Moreover, the same transcription factors have been implicated in the inhibition of generation of glial cells. Future molecular and genetic studies will be needed to elucidate the molecular mechanisms responsible for the Bcl-X_L effects described here.

In vivo, after transplantation into the aged rat striatum (to mimic the situation of a late-onset disease, with a preclinical orientation), grafts of Bcl-X_L overexpressing hNS1 cells survived better, and contained more neuronal cells and less glial cells than control hNS1 cell grafts. Similarly, mouse ES cells overexpressing Bcl-X_L showed a better reinnervation of the striatum of 6-OH-DA rats.[7] In the present work, it is important to note that Bcl-X_L did enhance hNSCs survival and neuronal differentiation, when implanted in a non-neurogenic site and, furthermore, impoverished, due to aging, for the supply of trophic factors such as brain-derived neurotrophic factor.[35] Therefore, Bcl-X_L seems to be able to override some of the tissue-imposed limitations for *in vivo* neuron generation by hNSCs.

In conclusion, in the context of hNSCs research, amounting data indicate that Bcl-X_L plays a major role in modulating the generation of neurons from both rodent- and human-derived stem cells,[7–10] and present work. Here, we contribute data indicating a more general role of Bcl-X_L, controlling the balance between the generation of neurons and glia from differentiating immortalized and non-immortalized hNSCs. In future work, it will be important to analyze the mechanisms of action of Bcl-X_L at the molecular level, and also the interaction of Bcl-X_L overexpressing cells with the surrounding environment after transplantation.

Materials and Methods

Cell culture

Cell lines of hNSCs. In this study, we have used control and Bcl-X_L overexpressing hNSCs derived from the hNS1 cell line (whose properties have been extensively described elsewhere).[8,27,28,30,37] This is a v-myc immortalized, non-transformed, human fetal forebrain-derived, multipotent, and clonal cell line of neural stem cells. hNS1 cell culture conditions are based on a chemically defined HSC-medium supplemented with 20 ng/ml of each epidermal growth factor (EGF) and basic fibroblast growth factor (FGF2).[27] Cells were proliferated at 5% CO_2 and normal atmospheric oxygen levels (resulting in 20% O_2). Cultures were differentiated on poly-L-lysine (10–50 μg/ml; Sigma) coated plastic or glass coverslips, by withdrawal of growth factors (EGF and FGF2) and addition of 0.5% heat-inactivated fetal bovine serum (FBS), for 12 days or the indicated times, at 5% O_2 and 5% CO_2 in a dual control O_2–CO_2 incubator (Forma).[8]

Non-immortalized forebrain hNSCs. Tissue was obtained from an aborted human fetus of 10 weeks gestational age (Lund University Hospital/Wallenberg Neuroscience Center; Dr Bengt Juliusson; Lund, Sweden). The tissue was donated for research after informed consent, and following EU directives, NECTAR recommendations, and Spanish law RD 42/1988. All procedures did follow Society for Neuroscience recommendations, and were also approved by the Bioethics of Research Committee of the University Autónoma of Madrid (Spain). Tissue pieces were digested to generate adherent primary cultures (2×10^5 cells per well of a 24-well plate), passed two times, and used for experimentation. Cells (secondary cultures) were grown as adherent cultures in the standard medium for hNSCs (i.e., under the influence of EGF and bFGF, 20 ng/ml each).

BrdU incorporation. To study cell proliferation during differentiation experiments, and Bcl-X_L effects on it, cultures were pulsed with BrdU (Sigma) under three different experimental designs.

Experiment 1: general cell proliferation rate. BrdU (10 μM) was applied for 2 h at days 0, 1, 3, 5, 7, 9, or 12 of the differentiation time course, and the cells were immediately fixed after the BrdU pulse for ICC.

Experiment 2: labeling of proliferating precursors that, after completion of the 12-day differentiation period, yielded β-III-tubulin$^+$ or GFAP$^+$ cells (birth dating). BrdU (1 μM) pulse was applied during 24 h at differentiation days 1, 3, 6, or 8 and the cells were let to differentiate until day 12 being subsequently fixed.

Experiment 3: proliferation of Nestin, β-III-tubulin, GFAP or vimentin precursors: BrdU (1 μM) was applied as in Experiment 2 but the cells were fixed immediately afterwards.

Bcl-X_L overexpression in hNSCs. The generation of stable Bcl-X_L overexpressing hNSCs (hNS1 subclone 5) was previously described.[8] Since continued Bcl-X_L expression in selected clones could result in changes in the cell's biology not directly linked to Bcl-X_L actions, we have also studied Bcl-X_L effects at a shorter time scale (days after transfection) (compare experiments shown in Figures 2 and 3). To this end, we infected control hNS1 cells with murine leukemia virus-derived, vesicular stomatitis virus glycoprotein pseudotyped retroviral vector stocks (generated in HEK 293 cells using the pVP-pack Stratagene system). Vectors had the following structure. *Control vector*: LTR-(empty)-IRES-RhGFP-LTR. *Bcl-X_L vector*: LTR-(Bcl-X_L)-IRES-RhGFP-LTR. (Rh-GFP stands for humanized *Renilla raniformis*-GFP.) *Rh-GFP* was subcloned into the retroviral backbone from the pFB-RhGFP plasmid. Titers were determined on HEK293 cells, and retroviral particles were used to infect hNS1 cells at a multiplicity of infection of one particle per cell. Cells were plated (day 0) in proliferation medium and differentiation was started at day 1. On day 2, cells were infected with retroviral stocks (prepared in Dulbecco's modified Eagle's medium/F-12 containing 5% FBS) for 4 h. After that, the regular differentiation medium was replaced, and the cells were let to differentiate until day 12.

For infection of non-immortalized forebrain hNSCs, cells were seeded at 2×10^5 cells/cm^2 (day 0) and infected in the same way as for hNS1, at day 1. On day 2, differentiation was started, by adding regular differentiation medium.

ICC and immunoblotting (WB). At the specified time points, the cultures were rinsed with PBS and fixed for 10 min in freshly prepared 4% PFA/PHEM/4% sucrose.[38] Cultures were blocked for 1 h in 10% normal horse serum, 0.25% Triton X-100 in PBS and incubated overnight at 4°C with mouse monoclonal antibodies against β-III-tubulin (1 : 1000; Sigma), GFAP (1 : 1000; Sigma), Nestin (1 : 500; Transduction Laboratories), vimentin (1 : 1000, Santa Cruz) and Map-2 (1 : 1000; Sigma) or monoclonal rat antibodies against BrdU (1 : 500; Abcam, UK) or rabbit antiserum against Ki-67 (1 : 3000; Lab Vision, UK), cleaved caspase-3 (1 : 100; Cell Signaling) synapsin-I (1 : 500; Chemicon) and GFAP (1 : 2000; DakoCytomation, Denmark).

On the next day, the cultures were incubated with biotinylated horse anti-mouse antibodies (1 : 200; Vector Laboratories) followed by streptavidin-CY3 (1 : 300, Jackson Immunoresearch) or FITC-conjugated antibodies (goat anti-rat, or -goat anti-rabbit, 1 : 200; Jackson Immunoresearch) or CY3-conjugated (goat anti-mouse; 1 : 300, Jackson Immunoresearch) or CY5-conjugated antibodies (donkey anti-rabbit; 1 : 300, Jackson Immunoresearch. For non-fluorescent ICC, samples were developed using the Vector ABC kit followed by diaminobenzidine (DAB) development. Cell nuclei were counterstained with Hoechst 33258 (Molecular Probes, Eugene, OR, USA) at 0.2 μg/ml in PBS. For BrdU ICC, before incubation with the first antibody, fixed cultures were treated with 2 M HCl at 37°C for 30 min, followed by three rinses in 0.1 M borate buffer (pH 8.9). For double ICC for BrdU and other antigens, BrdU processing and staining was performed as a second ICC round. Cell nuclei staining in BrdU ICCs was performed using propidium iodide (PI; Sigma) (1 μg/ml in PBS) at the end of the staining process. For western analysis, 30 μg of protein from dividing or differentiated cultures were assayed. Samples were electrophoresed and transferred to nitrocellulose membranes overnight. Primary antibodies were mAb anti-β-actin (1 : 5000; Sigma) and rabbit polyclonal anti-Bcl-X_L (1 : 1000; Transduction Laboratories). The blots were developed using peroxidase-conjugated horse anti-mouse (horse anti-mouse peroxidase (HAMPO), 1 : 5000; Vector Laboratories) or goat anti-rabbit antibodies (goat anti-rabbit peroxidase (GARPO), 1 : 10 000; Nordic Immune) and developed using the ECL system (Amersham Biosciences, Arlington Heights, IL, USA).

Cell death. To study cell death parameters during differentiation of hNS1 and Bcl-X_L overexpressing cells, we performed the following experiments combining different techniques:

(a) The number of alive and dying–dead cells was quantified in alive cultures stained with calcein-AM/PI (1 μM calcein-AM (Molecular Probes) and 4 μM PI (Sigma)). Cells were stained for 15 min at 37°C and photographed, for offline quantification. Green cells are alive cells, while red-stained nuclei identify dead or dying cells.

(b) Analysis of Annexin V$^+$ cells, and nuclear morphology: phosphatidylserine exposure on the outer leaflet of the plasma membrane[39] was detected using the fluorescent dye Annexin V-CY5 (Annexin-V-CY5 detection Kit (Abcam) according to the manufacturer's instructions. In brief, at specified time points culture medium was replaced by Annexin V binding buffer, then 1 μl of Annexin V-CY5 antibody was added and the cells were incubated in this solution for 5 min at room temperature. Nuclei were counterstained with Hoechst 33258 (Molecular Probes, 0.2 μg/ml in PBS, for 10 min). Dying–dead cells were identified by showing a condensed or fragmented nucleus.

(c) Determination of the sub-G_0/G_1 cell population by flow cytometry:[40] cells were trypsinized, washed in PBS, fixed with 70% ethanol at -20°C, and stored at -20°C until all the time points were collected. At the time of analysis, cells were incubated in the staining solution for 30 min at 37°C (PBS containing 0.1% of sodium citrate, 0.3% of NP-40, 0.02 mg/ml of RNase, and 0.05 mg/ml of PI (Sigma)). DNA content was determined using a fluorescence-activated cell sorter, FACS Calibur flow cytometer (BD Bioscience). A total of 10 000 events were acquired per sample and data were analyzed by CellQuest Software (BD Bioscience).

Image and data analyses on cell cultures. Analyses and photography of fluorescent- or DAB-immunostained cultures were carried out in an inverted Zeiss (Oberkochen, Germany) Axiovert 135 or Leica (Nussloch, Germany) DM IRB (equipped with a digital camera Leica DC100) microscopes. In some experiments, digitized images were captured using Leica IM500 Software. Image analyses were performed using NIH Image Software. Statistical tests were run using Prophet Software (NIH). Results are shown as the average $\pm$ S.E.M. of data from four to five experiments, unless stated otherwise.

***In vivo* transplantation.** Aged female Wistar rats (23 months old), housed and treated according to the European Community guidelines (86/609/EEC) were anesthetized with a mix of Ketamine and Dontor, and grafted onto the right striatum with cellular suspensions of proliferating control hNS1 cells ($n = 5$) or Bcl-X_L–hNS1 cells ($n = 5$), at the following coordinates (in mm, tooth bar set at -2.3): antero-posterior (AP) $= +1$; medio-lateral (ML) $= -3$; dorso-ventral (DV) (from dura) $= -4.5$. A total of 400 000 cells were implanted as a single deposit (cell density of 150–200 000 cells/μl). The animals were immune suppressed with cyclosporine A (Neoral; Novartis) at 100 μg/ml in drinking water, starting 48 h before grafting. Four weeks after grafting, rats were intracardially perfused with freshly prepared, buffered 4% paraformaldehyde. Brains were post-fixed for 12 h, dehydrated in 30% sucrose, and sectioned (30 μm, freezing microtome) for free-floating immunohistochemistry analyses. Serial sections were processed for monoclonal anti-hNuc (MAB 1281; 1 : 500; Chemicon) to detect all grafted and surviving human cells. Migrating neuroblasts and immature neurons were detected using anti-Dcx antibodies (C-18; 1 : 1000; Santa Cruz Biotechnology), and human neurons were specifically stained using an anti-human neuron-specific enolase antibody (MAB324; 1 : 2000; Chemicon). Undifferentiated cells were detected using polyclonal anti-Nestin antibody (1 : 1000; Abcam). Astroglial cells were stained with a polyclonal antibody anti-GFAP (1 : 2000; Dako, Denmark). For the unambiguous detection of GFAP, Nestin, or Dcx in human cells, double IHC was performed combining these antibodies with those for hNuc. Secondary antibodies were biotinylated horse anti-mouse (1 : 200; BA2001; Vector Laboratories), followed by ABC (Vector Laboratories) and Ni–DAB reaction. For immunofluorescence (IF) secondary antibodies were conjugated to Texas Red (horse anti-mouse; 1 : 100; Vector Laboratories), Alexa 488 (goat anti-rabbit; 1 : 400; Molecular Probes), or FITC (donkey anti-goat; 1 : 200; Jackson Immunoresearch).

Single IF or DAB sections were analyzed on a Leica DM IRB inverted fluorescence microscope. For double IF analyses, sections were analyzed on a Microradiance Confocal microscope (Bio-Rad, Hercules, CA, USA). To determine the phenotype of transplanted cells, hNuc$^+$ cells double immunostained for Nestin, Dcx, or GFAP, were analyzed in confocal z axis serial images (at 63 $\times$ magnification). A total of 3–4 sections per animal ($n = 3$ in control group and $n = 4$ in Bcl-X_L group) and between 300 and 500 cells per section were analyzed. For

each hNuc$^+$ cell, the complete cell nucleus was scanned through the *z* axis, and only cells with a well circumscribed, immunopositive cell body or nucleus were considered positive for a particular phenotype. Orthogonal projections and volume quantifications were done from low magnifications (25 $\times$, 40 $\times$) *z* images (0.5–1 μm thickness) using Metamorph software (Universal Imaging Corporation, West Chester, PA, USA).

Acknowledgements. This work was supported by grants from the European Union (QLK3-CT-2001–02120), Spanish Ministry of Science and Technology (MCYT – SAF2001-0841 and SAF2004-03405) and Comunidad Autonoma de Madrid (GR/SAL/0115/2004). The Institutional grant from Foundation Ramón Areces to the Center of Molecular Biology Severo Ochoa (CBMSO) is also gratefully acknowledged. We thank Dr. B Juliusson (Lund University Hospital) for providing human neurospheres for control experiments, and Dr. P Kusk (NsGene A/S, Denmark) for retroviral vectors. IL was supported by QLK3-CT-2001–02120 and the Comunidad Autónoma de Madrid. EGG and C Bueno are recipients of fellowships from the Spanish Ministry of Education. The excellent technical assistance of Bárbara B Sese, Inmaculada Ocaña, and Juliana Sánchez is also gratefully acknowledged.

1. Lindvall O, Kokaia Z, Martinez-Serrano A. Stem cell therapy for human neurodegenerative disorders – how to make it work. *Nat Med* 2004; **10**: S42–S50.
2. Goldman S. Stem and progenitor cell-based therapy of the human central nervous system. *Nat Biotechnol* 2005; **23**: 862–871.
3. Suzuki M, Wright LS, Marwah P, Lardy HA, Svendsen CN. Mitotic and neurogenic effects of dehydroepiandrosterone (DHEA) on human neural stem cell cultures derived from the fetal cortex. *Proc Natl Acad Sci USA* 2004; **101**: 3202–3207.
4. Hsieh J, Nakashima K, Kuwabara T, Mejia E, Gage FH. Histone deacetylase inhibition-mediated neuronal differentiation of multipotent adult neural progenitor cells. *Proc Natl Acad Sci USA* 2004; **101**: 16659–16664.
5. Laeng P, Pitts RL, Lemire AL, Drabik CE, Weiner A, Tang H *et al.* The mood stabilizer valproic acid stimulates GABA neurogenesis from rat forebrain stem cells. *J Neurochem* 2004; **91**: 238–251.
6. Lie DC, Colamarino SA, Song HJ, Desire L, Mira H, Consiglio A *et al.* Wnt signaling regulates adult hippocampal neurogenesis. *Nature* 2005; **437**: 1370–1375.
7. Shim JW, Koh HC, Chang MY, Roh E, Choi CY, Oh YJ *et al.* Enhanced *in vitro* midbrain dopamine neuron differentiation, dopaminergic function, neurite outgrowth, and 1-methyl-4-phenylpyridium resistance in mouse embryonic stem cells overexpressing Bcl-X_L. *J Neurosci* 2004; **24**: 843–852.
8. Liste I, Garcia-Garcia E, Martinez-Serrano A. The generation of dopaminergic neurons by human neural stem cells is enhanced by Bcl-X_L, both *in vitro* and *in vivo*. *J Neurosci* 2004; **24**: 10786–10795.
9. Savitt JM, Jang SS, Mu W, Dawson VL, Dawson TM. Bcl-x is required for proper development of the mouse substantia nigra. *J Neurosci* 2005; **25**: 6721–6728.
10. Chang MY, Sun W, Ochiai W, Nakashima K, Kim SY, Park CH *et al.* Bcl-XL /Bax proteins direct the fate of embryonic cortical precursor cells. *Mol Cell Biol* 2007; **27**: 4293–4305.
11. Gonzalez-Garcia M, Garcia I, Ding L, O'Shea S, Boise LH, Thompson CB *et al.* Bcl-x is expressed in embryonic and postnatal neural tissues and functions to prevent neuronal cell death. *Proc Natl Acad Sci USA* 1995; **92**: 4304–4308.
12. Krajewska M, Mai JK, Zapata JM, Ashwell KW, Schendel SL, Reed JC *et al.* Dynamics of expression of apoptosis-regulatory proteins Bid, Bcl-2, Bcl-X, Bax and Bak during development of murine nervous system. *Cell Death Differ* 2002; **9**: 145–157.
13. Benn SC, Woolf CJ. Adult neuron survival strategies: slamming on the brakes. *Nat Rev Neurosci* 2004; **5**: 686–700.
14. Jordan J, Galindo MF, Tornero D, Gonzalez-Garcia C, Cena V. Bcl-x L blocks mitochondrial multiple conductance channel activation and inhibits 6-OHDA-induced death in SH-SY5Y cells. *J Neurochem* 2004; **89**: 124–133.
15. Motoyama N, Wang F, Roth KA, Sawa H, Nakayama K, Nakayama K *et al.* Massive cell death of immature hematopoietic cells and neurons in Bcl-x-deficient mice. *Science* 1995; **267**: 1506–1510.
16. Parsadanian AS, Cheng Y, Keller-Peck CR, Holtzman DM, Snider WD. Bcl-xL is an antiapoptotic regulator for postnatal CNS neurons. *J Neurosci* 1998; **18**: 1009–1019.
17. Li C, Fox CJ, Master SR, Bindokas VP, Chodosh LA, Thompson CB. Bcl-X(L) affects Ca(2+) homeostasis by altering expression of inositol 1,4,5-trisphosphate receptors. *Proc Natl Acad Sci USA* 2002; **9**: 9830–9835.
18. Jonas EA, Hoit D, Hickman JA, Brandt TA, Polster BM, Fannjiang Y *et al.* Modulation of synaptic transmission by the BcL-2 family protein BCL-xL. *J Neurosci* 2003; **23**: 8423–8431.
19. Zinkel S, Gross A, Yang E. Bcl2 family in DNA damage and cell cycle control. *Cell Death Differ* 2006; **13**: 1351–1359.
20. Limana F, Urbanek K, Chimenti S, Quaini F, Leri A, Kajstura J *et al.* Bcl-2 overexpression promotes myocyte proliferation. *Proc Natl Acad Sci USA* 2002; **9**: 6257–6262.
21. Sommer L, Rao M. Neural stem cells and regulation of cell number. *Prog Neurobiol* 2002; **66**: 1–18.
22. Ostenfeld T, Svendsen CN. Requirement for neurogenesis to proceed through the division of neuronal progenitors following differentiation of epidermal growth factor and fibroblast growth factor-2-responsive human neural stem cells. *Stem Cells* 2004; **22**: 798–811.
23. Martinez-Serrano A, Rubio FJ, Navarro B, Bueno C, Villa A. Human neural stem and progenitor cells: *in vitro* and *in vivo* properties, and potential for gene therapy and cell replacement in the CNS. *Curr Gene Ther* 2001; **1**: 279–299.
24. Ourednik V, Ourednik J, Flax JD, Zawada WM, Hutt C, Yang C *et al.* Segregation of human neural stem cells in the developing primate forebrain. *Science* 2001; **293**: 1820–1824.
25. Tabar V, Panagiotakos G, Greenberg ED, Chan BK, Sadelain M, Gutin PH *et al.* Migration and differentiation of neural precursors derived from human embryonic stem cells in the rat brain. *Nat Biotechnol* 2005; **23**: 601–606.
26. Kee N, Sivalingam S, Boonstra R, Wojtowicz JM. The utility of Ki-67 and BrdU as proliferative markers of adult neurogenesis. *J Neurosci Methods* 2002; **115**: 97–105.
27. Villa A, Snyder EY, Vescovi A, Martinez-Serrano A. Establishment and properties of a growth factor-dependent, perpetual neural stem cell line from the human CNS. *Exp Neurol* 2000; **161**: 67–84.
28. Villa A, Navarro-Galve B, Bueno C, Franco S, Blasco MA, Martinez-Serrano A. Long-term molecular and cellular stability of human neural stem cell lines. *Exp Cell Res* 2004; **294**: 559–570.
29. Rubio FJ, Bueno C, Villa A, Navarro B, Martinez-Serrano A. Genetically perpetuated human neural stem cells engraft and differentiate into the adult mammalian brain. *Mol Cell Neurosci* 2000; **16**: 1–13.
30. Navarro-Galve B, Villa A, Bueno C, Thompson L, Johansen J, Martinez-Serrano A. Gene marking of human neural stem/precursor cells using green fluorescent proteins. *J Gene Med* 2005; **7**: 18–29.
31. Lindsten T, Golden JA, Zong WX, Minarcik J, Harris MH, Thompson CB. The proapoptotic activities of Bax and Bak limit the size of the neural stem cell pool. *J Neurosci* 2003; **23**: 11112–11119.
32. Nieto M, Schuurmans C, Britz O, Guillemot F. Neural bHLH genes control the neuronal *versus* glial fate decision in cortical progenitors. *Neuron* 2001; **29**: 401–413.
33. Sun Y, Nadal-Vicens M, Misono S, Lin MZ, Zubiaga A, Hua X *et al.* Neurogenin promotes neurogenesis and inhibits glial differentiation by independent mechanisms. *Cell* 2001; **104**: 365–376.
34. Horton S, Meredith A, Richardson JA, Johnson JE. Correct coordination of neuronal differentiation events in ventral forebrain requires the bHLH factor MASH1. *Mol Cell Neurosci* 1999; **14**: 355–369.
35. Collier TJ, Sortwell CE, Daley BF. Diminished viability, growth, and behavioral efficacy of fetal dopamine neuron grafts in aging rats with long-term dopamine depletion: an argument for neurotrophic supplementation. *J Neurosci* 1999; **19**: 5563–5573.
36. Peterson DA, Gnatenco C, Peterson LD. The aged brain exhibits impaired capacity to support neurogenesis. *Exp Neurol* 2003; **181**: 102–103.
37. Liste I, Navarro B, Johansen J, Bueno C, Villa A, Johansen TE *et al.* Low-level tyrosine hydroxylase (TH) expression allows for the generation of stable TH$^+$ cell lines of human neural stem cells. *Hum Gene Ther* 2004; **15**: 13–20.
38. Tejero-Diez P, Rodriguez-Sanchez P, Martin-Cofreces NB, Diez-Guerra FJ. bFGF stimulates GAP-43 phosphorylation at ser41 and modifies its intracellular localization in cultured hippocampal neurons. *Mol Cell Neurosci* 2000; **16**: 766–780.
39. Tamm C, Robertson JD, Sleeper E, Enoksson M, Emgard M, Orrenius S *et al.* Differential regulation of the mitochondrial and death receptor pathways in neural stem cells. *Eur J Neurosci* 2004; **19**: 2613–2621.
40. Kanzawa T, Iwado E, Auki H, Iwamaru A, Hollingsworth EF, Sawaya R *et al.* Ionizing radiation induces apoptosis and inhibits neuronal differentiation in rat neural stem cells via c-Jun NH2-terminal kinase (JNK) pathway. *Oncogene* 2006; **25**: 3638–3648.

Supplementary Information accompanies the paper on Cell Death and Differentiation website (http://www.nature.com/cdd)